

Structure, Energetics, Electronic, and Hydration Properties of Neutral and Anionic Al₃O₆, Al₃O₇, and Al₃O₈ Clusters

S. Gowtham, Kah Chun Lau, Mrinalini Deshpande,* and Ravindra Pandey

Department of Physics, Michigan Technological University, Houghton, Michigan 49931

Anita K. Gianotto and Gary S. Groenewold

Idaho National Engineering and Environmental Laboratory, Idaho Falls, Idaho 83415

Received: December 30, 2003; In Final Form: March 26, 2004

We report the results of a theoretical study of neutral and anionic Al₃O_n ($n = 6-8$) and an experimental investigation of Al₃O₆H₂⁻ clusters, focusing on their structural and electronic properties. Our results, based on density functional calculations, reveal that sequential oxidation of Al₃O₅ induces significant structural changes in the cluster configurations in which an O₂ molecule tends to replace an O atom. The neutral Al₃O_n ($n = 6-8$) clusters are found to be in doublet electronic states, with a planar to three-dimensional close-packed structure being most stable. The triplet state is found to be the optimum electronic state for the ground state of anionic Al₃O_n ($n = 6-8$). The clusters showed an energetic preference for a twisted-pair rhombic structure, although for $n = 6$ and 8, a planar hexagonal structure was only 0.16 eV higher in energy. It is also shown that the strength of the oxygen–oxygen bond dominates the preferred fragmentation path for both neutral and anionic clusters. The hydration behavior of an $n = 6$ cluster Al₃O₆H₂⁻ was examined experimentally using an ion trap–secondary ion mass spectrometer under vacuum conditions, and the gas-phase clusters were shown to add three H₂O molecules. Since H₂O addition is consistent with the presence of under-coordinated metals in oxide clusters, the experimental result for $n = 6$ was consistent with the planar hexagonal structure, which contained three under-coordinated Al sites.

I. Introduction

Aluminum oxide, Al₂O₃, traditionally referred to as alumina, is a very important ceramic material that has many technological applications. Its great usefulness as a ceramic material rests primarily on its extreme hardness (15 Gpa), high melting point (2327 K), and low electrical conductivity (10⁻¹² S/m at 20 °C). It has a wide range of applications, from electronics, optics, biomedical, and mechanical engineering to catalyst support. In the bulk Al₂O₃, bonding interactions are chiefly ionic.¹ The valence electrons of aluminum (i.e. 3s²3p¹) are transferred to oxygen, thus producing closed shell Al³⁺ and O²⁻ ions whose electrostatic interactions are primarily responsible for alumina's cohesive energy. Clusters of aluminum oxide have, consequently, been studied both theoretically and experimentally to better understand the relationship between structure and bonding between aluminum and oxygen.

In Al_mO_n clusters,^{2,3} for a given m , transformation from metallic to ionic bonding was observed with increasing n . As an example of hypermetalated species, Al₃O was considered for theoretical calculations.^{4,5} Quantum mechanical calculations on neutral and anionic Al₃O_n ($n \leq 5$) have shown how structure reflects ionic bonding and localization of electrons on aluminum atoms.⁶⁻¹¹ There have been many experimental studies^{2,3} of small aluminum–oxygen clusters, including a systematic photoelectron spectroscopy study of Al₃O_n⁻ ($n = 0-5$). Wu et al.³ reported that the sequential oxidation of Al₃ has led to a higher value of the electron affinity. For Al₃O₅⁻, the photoelectron

spectrum suggests a complete transfer of valence electrons from Al to O in the cluster. Additionally, calculations based on the electron propagator method⁷ for Al₃O₅ and Al₃O₅⁻ find that Dyson orbitals associated with the lowest electron detachment energies are dominated by p functions on terminal oxygens in the cluster.

Recent mass spectrometry studies conducted by Groenewold and co-workers showed that alumina clusters were formed by projectile bombardment of alumina surfaces using an ion trap–secondary ion mass spectrometer (IT-SIMS).^{12,13} The approach could not provide any direct insight into the electronic structure of the clusters formed, but it did show that the reactivity with respect to H₂O and H₂S could be readily studied. The results of the reactivity studies might be correlated with structure if the same systems were studied.

In the present study, we now investigate the effect of sequential oxidation of Al₃O₅ on structural and electronic properties of the oxygen-rich alumina clusters. We focus on neutral and anionic Al₃O_n, ($n = 6-8$) clusters and report here their equilibrium properties, including configurational parameters, binding and fragmentation energies, vibrational frequencies, highest occupied molecular orbital (HOMO)–lowest unoccupied molecular orbital (LUMO) gap, and electron affinity (EA). It is noted that none of the previous experimental and theoretical studies considered Al₃O_n for $n \geq 5$. Therefore, the work presented here provides new results and insight into the structure and bonding of Al₃O_n ($n = 6-8$), enabling us to assess both size and charge dependence of the structural properties at the same level of theory. We also present experimental results describing the extent of hydration observed for Al₃O₆H₂⁻ species

* Permanent Address: Department of Physics, H. P. T. Arts and R. Y. K. Science College, Nasik, India.

that are formed in the gas-phase atmosphere of the IT-SIMS, which will enable reactivity to be discussed in the context of the computational structural possibilities.

The rest of the paper is organized as follows. In section II, we give a brief description of the computational and experimental methods used in this work. The results are presented and discussed in section III, and in section IV we give the summary of the results of this work.

II. Computational and Experimental Details

A. Computational Details. The electronic structure calculations were performed on neutral and negative Al_3O_n ($n = 6-8$) clusters in the framework of density functional theory (DFT) using the Gaussian 98 program suite.¹⁴ Total energy calculation of a given cluster configuration was performed using the hybrid B3LYP exchange and correlation functional with the 6-31G** (i.e. 6-31G(d,p)) basis set for Al and O in this study. The geometry optimizations on symmetry-constrained multidimensional potential energy surfaces were achieved with a gradient norm smaller than 10^{-6} hartree/bohr and an energy convergence of 10^{-8} hartree. Different spin multiplicities for the given cluster configuration were considered as well. Since neutral Al_3O_n clusters have an odd number of valence electrons and anionic Al_3O_n clusters have an even number of valence electrons, doublet/quartet and singlet/triplet spin states were considered for neutral and anionic clusters, respectively. For the lowest energy cluster configuration, the vibrational frequencies under harmonic approximation were also computed to assess the stability of the cluster configuration.

To benchmark the modeling elements (e.g. basis sets) of the present study, we began with the Al_3O_5 cluster, which was the focus of a previous electronic structure study by Martínez et al.⁷ They performed DFT and QCISD calculations on neutral and anionic Al_3O_5 using the 6-311+G(2d) basis set for Al and O atoms. The calculated results of Martínez et al.⁷ find a nonplanar basket-like structure to be the ground state of neutral Al_3O_5 . For anionic Al_3O_5 , they predict a planar windowpane structure to be the ground state. On the other hand, the results of the photoelectron study³ suggest either a kite or an open windowpane configuration for the ground state of the neutral Al_3O_5 cluster. In the present study, the predicted ground-state configurations for neutral and anionic Al_3O_5 are in agreement with those predicted by the DFT/QCISD study,⁷ though we use the 6-31G(d,p) basis set for Al and O atoms. It is to be noted here that the same B3LYP-DFT functional was used in both theoretical studies.

B. Experimental Details. Hydration studies were performed using an ion trap—secondary ion mass spectrometer (IT-SIMS) that has been described previously and has been used in numerous reactivity studies.^{12,13,15-18} Briefly, $\text{Al}_x\text{O}_y\text{H}_z^-$ cluster ions are generated by bombarding the surface of alumina with an energetic molecular ion beam. The cluster ions are subsequently mass selected and then allowed to react with gaseous neutrals within the instrument. Finally, the reaction product ions are scanned out and detected. The IT-SIMS base pressure was typically 2×10^{-8} Torr, and a variable leak valve was used to admit $\sim 3 \times 10^{-7}$ Torr H_2O for hydration studies. After the H_2O was admitted, He bath gas needed for trajectory damping in the IT was added, so that the total pressure was 7×10^{-6} Torr. The relative partial pressures were monitored with an Inficon residual gas analyzer connected to the vacuum manifold.

The gas-phase $\text{Al}_x\text{O}_y\text{H}_z^-$ ions were produced from powdered aluminum (oxy) hydroxide (synthetically prepared by D. A. Cummings, INEEL). XRD analyses confirmed the prepared sample as a mixture of Gibbsite and Bayerite ($\text{Al}(\text{OH})_3$). The

sputtered $\text{Al}_x\text{O}_y\text{H}_z^-$ ions were then trapped in the IT-SIMS, where they subsequently reacted with the gaseous H_2O .

The IT-SIMS was based on a modified Varian Saturn 2000 ITMS (Walnut Creek, CA) previously described in the literature.¹⁹⁻²¹ The instrument was equipped with a ReO_4^- primary ion beam that is more efficient for sputtering cluster ions into the gas phase relative to atomic particle bombardment.²²⁻²⁵ The ReO_4^- ion gun was operated at 7.0 keV, at a primary ion current of ~ 1200 pA. The typical ionization time for generating $\text{Al}_x\text{O}_y\text{H}_z^-$ was 200 ms. Secondary ions sputtered from the sample surface were focused into the ion trap using a small cylindrical electrostatic lens, which also served to mitigate charge buildup on the bombarded sample surface.²⁶ During the ionization period, the reactant ions of interest ($\text{Al}_3\text{O}_6\text{H}_2^-$ and $\text{Al}_3\text{O}_7\text{H}_4^-$) were isolated using selected ion storage,²⁷ which resulted in ejection of unwanted ions on the basis of their mass-dependent motional frequencies. Isolated ions were then allowed to react with H_2O during a specified reaction time (0–10 s) that was systematically controlled. The ion trap was operated at a low mass cutoff of 55μ during the ionization time period. During the isolation and reaction time periods, the low mass cut off was set at a q_z value of 0.7. Finally, the ionic reactants and products were scanned out of the trap²⁷ for detection. A diagram of the instrument can be found in a previous paper.¹⁹

III. Results and Discussion

A. Structural Properties. Several planar and nonplanar configurations of neutral and anionic Al_3O_6 , Al_3O_7 , and Al_3O_8 clusters were considered for the symmetry-constrained geometry optimization. Figure 1 presents a schematic picture of the different isomers considered in this study for Al_3O_6 . The choice of each of these isomers was partially based on the previous DFT study of Al_3O_5 ,⁷ Al_3O_4 ,⁹ and Si_3O_6 .²⁸

Some of the low-energy structures obtained from DFT calculations for both neutral and anionic Al_3O_n ($n = 6-8$) clusters are given in Figures 2–4 with the energies relative to the most stable isomer. The ground state of neutral Al_3O_6 prefers a planar hexagonal structure; this motif is also seen in the low-energy neutral Al_3O_7 and Al_3O_8 structures, although in these cases addition of more O atoms results in O above and below the plane of the Al_3O_3 hexagon. As the molecule becomes more oxidized, undistorted trigonal planar Al atoms are converted to tetrahedral geometry. In the negatively charged state, clusters are found to prefer configurations where Al and O atoms form twisted-pair rhombus structures. We note here that the ground state of the neutral clusters is doublet, while that of anionic clusters is triplet.

Al_3O_6 . Several initial configurations of Al_3O_6 are considered for DFT calculations (Figure 1). The lowest energy configuration is identified as a hexagonal planar (C_{2v} symmetry) geometry with a doublet spin state and is schematically shown in Figure 2. It consists of a six-membered ring with three aluminum and three oxygen atoms. Three exocyclic oxygen atoms are attached with three Al atoms at apex positions. In this structure, the three Al atoms are surrounded by the six O atoms, which is the most favorable arrangement from a simple electrostatic consideration. In the ring, $R_{\text{Al-O}}$ (i.e. Al–O bond distance) is about 1.71 Å, while the bond distance of Al to the exocyclic oxygen is about 1.75 Å. We note here that $R_{\text{Al-O}}$ in the AlO molecule is reported²⁹ to be 1.67 Å. The energy difference between doublet and quartet spin states for the lowest energy configuration is calculated to be 0.36 eV.

The next lowest energy structure for neutral Al_3O_6 is higher in energy by about 0.73 eV than the ground state. This three-dimensional (3D) structure can be viewed as a distorted

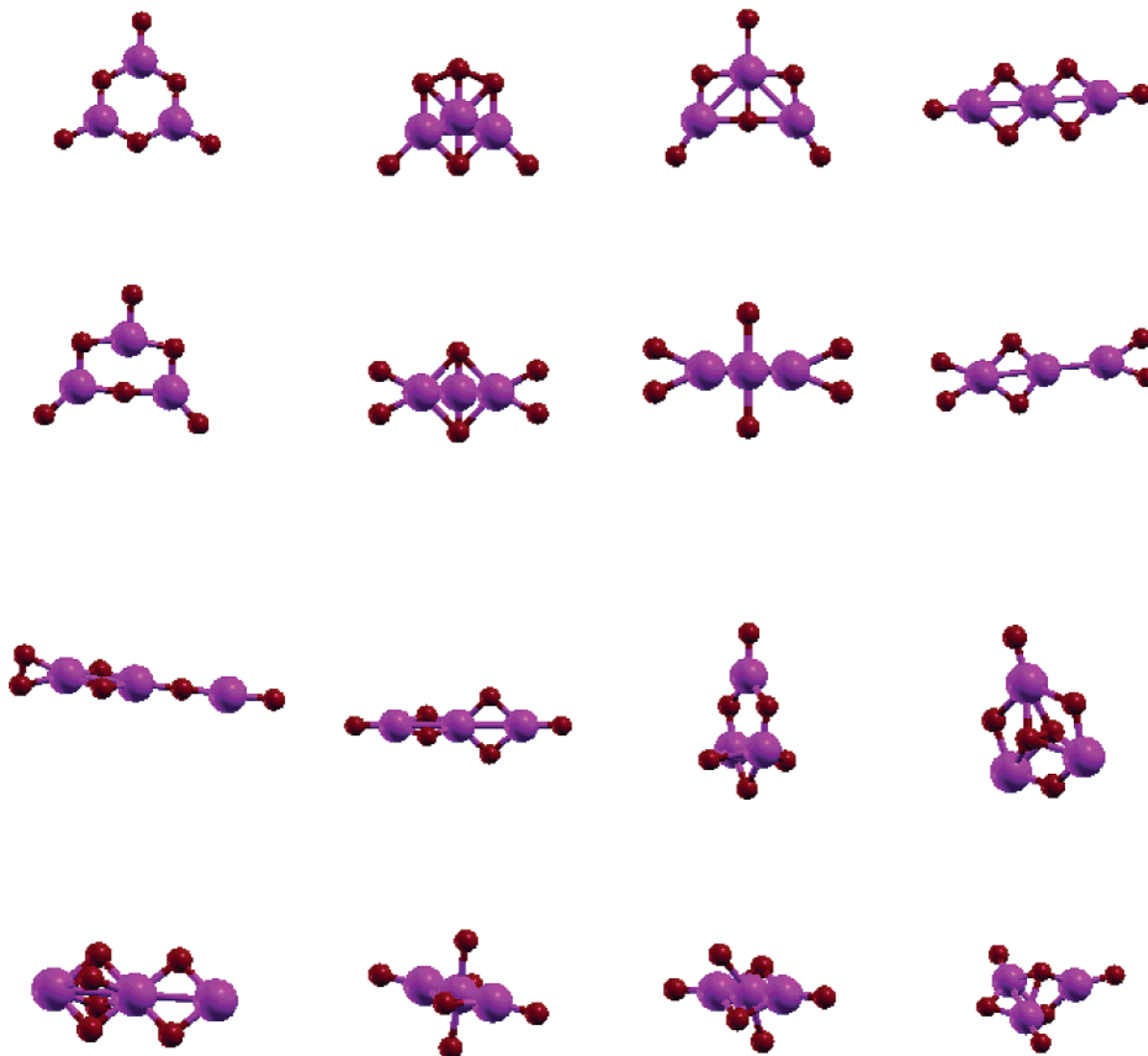


Figure 1. Schematic representation of different isomers considered in this study for Al_3O_6 . Aluminum and oxygen atoms are represented by large and small filled circles, respectively.

windowpane structure predicted for Al_3O_5 ,⁷ where one of the Al atoms is coordinated by four oxygen neighboring atoms. It also shows the presence of an O_2 unit with $R_{\text{O}-\text{O}}$ of 1.56 Å. Above this energy level, a competition between two-dimensional (2D) and three-dimensional structures for the stable oxygen-rich clusters starts to emerge. The next isomer, which is 0.89 eV higher than the ground state, is formed by addition of the sixth oxygen atom to the neutral ground-state (basket-like) structure of Al_3O_5 .⁷ It also shows the presence of an O_2 unit with $R_{\text{O}-\text{O}}$ of 1.53 Å. Finally, a structure similar to the ground-state structure of Si_3O_6 ²⁸ is predicted to be 1.32 eV higher in energy. Here, two Al_2O_2 rhombuses share a central Al atom, forming a twisted-pair rhombus structure with $R_{\text{Al}-\text{O}}$ of about 1.75 Å.

The addition of an electron to Al_3O_6 affects the configuration symmetry of the lowest lying structure of neutral Al_3O_6 . For anionic Al_3O_6 , the most stable configuration is a triplet nonplanar configuration with C_1 symmetry. It consists of a twisted pair of Al_2O_2 rhombuses sharing a central Al atom (Figure 2). The calculated singlet–triplet splitting is 1.55 eV. There is a very small change in $R_{\text{Al}-\text{O}}$ in the anionic cluster relative to that in the neutral cluster. The second most stable isomer bears a strong resemblance to the ground state of the neutral configuration with C_{2v} symmetry and is predicted to be 0.16 eV higher in energy. The next low-lying singlet configura-

tions are nonplanar structures containing O_2 units and are about 1.55–1.58 eV higher in energy. Here, $R_{\text{Al}-\text{O}}$ remains least affected by the addition of an electron.

Al_3O_7 . Addition of one oxygen to the neutral Al_3O_6 cluster leads to a 3D configuration with C_{2v} symmetry (Figure 3). The resulting configuration can be viewed as an O_2 unit attached to Al_3O_5 via an Al atom with $R_{\text{Al}-\text{O}}$ of 1.86 Å. In the O_2 unit, $R_{\text{O}-\text{O}}$ is 1.37 Å, indicating the presence of a stronger O–O bond in the cluster. The calculated doublet–quartet splitting is 0.36 eV. The next isomer is a nonplanar twisted-pair Al_2O_2 rhombus structure with terminating O atom at one end and an O_2 unit at the other. It is 1.31 eV higher in energy and bears a strong resemblance to the ground state of the anionic Al_3O_6 structure. The other nonplanar configurations, as shown in Figure 3, are about 1.6 and 1.96 eV higher in energy.

For anionic Al_3O_7 , a nonplanar twisted-pair rhombus structure is the lowest energy structure. Here, the singlet configuration lies approximately 1.72 eV above the triplet configuration. There are two more triplet configurations that are 0.14 and 0.32 eV higher in energy, respectively, in which three Al and three O atoms form a distorted ringlike structure. Somewhat higher in energy (1.06 eV), there is a planar structure, similar to the ground state of Al_3O_6 . All the isomers of Al_3O_7^- considered here contain an O_2 unit with $R_{\text{O}-\text{O}}$ of about 1.4–1.6 Å.

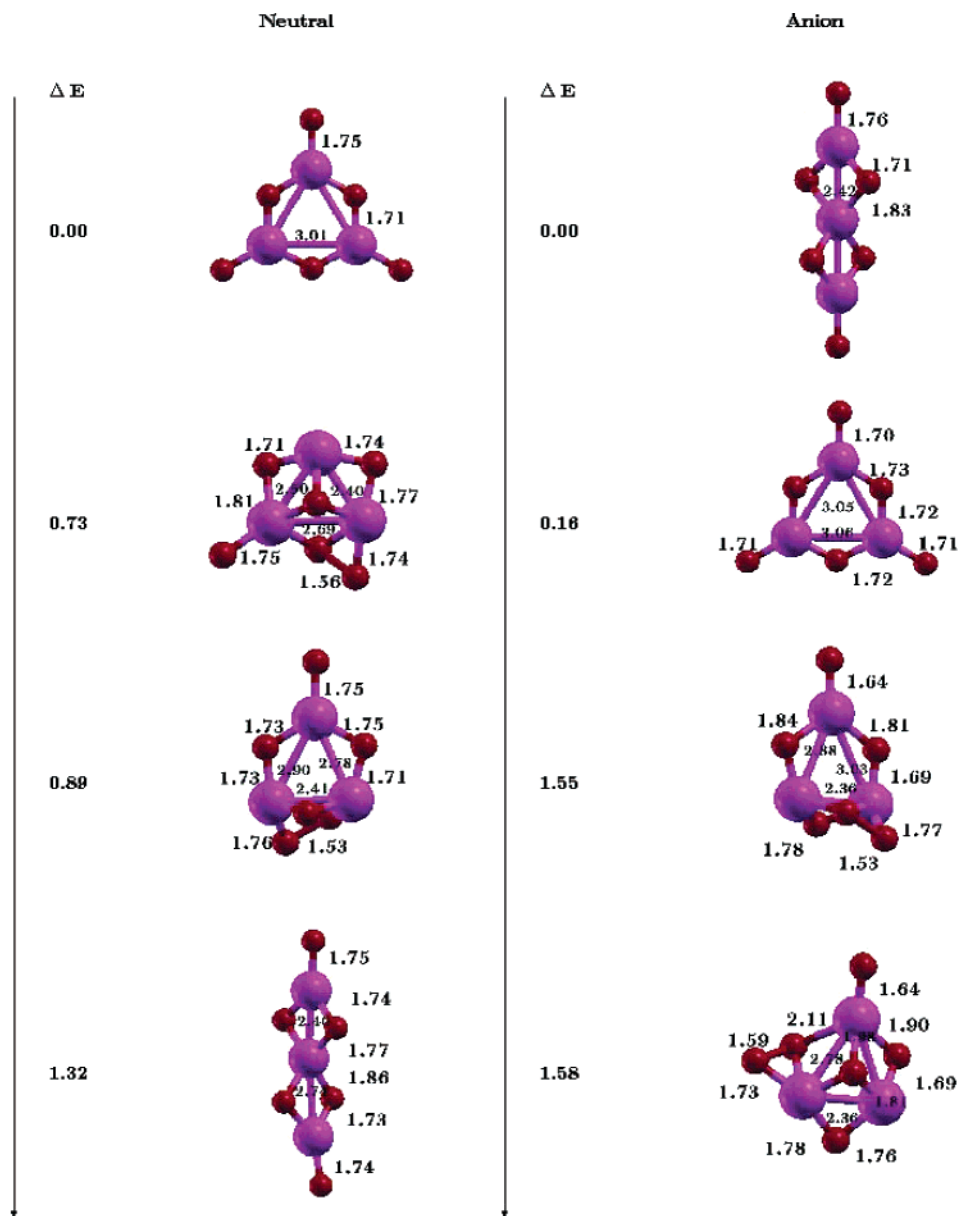


Figure 2. Some of the lowest energy configurations of neutral and anionic Al_3O_6 . Energy difference is in eV. Aluminum and oxygen atoms are represented by large and small filled circles, respectively.

Al_3O_8 . In Al_3O_8 , a six-membered ring with two bound O_2 units is the lowest energy structure in which one of the terminal O atom of neutral Al_3O_7 structure (Figure 4) is replaced by an additional O_2 . The doublet and quartet spin states are found to be nearly degenerate for this cluster configuration. As shown in Figure 4, the twisted-pair rhombus structure lays 1.40 eV above the ground state. In the O_2 unit, $R_{\text{O}-\text{O}}$ is about 1.4 Å, suggesting the formation of an O_2 molecule. We may therefore view the ground state of Al_3O_8 as $\text{O}_2-\text{Al}_3\text{O}_4-\text{O}_2$.

In anionic Al_3O_8 , there are two stable triplet structures with an energy difference of 0.16 eV. The most stable configuration has the twisted-pair rhombus structure, while the next lowest structure resembles the neutral ground state. A stable singlet state was found, but it was 2.59 eV higher in energy than the lowest triplet state (Figure 4).

Al_3O_n ($n = 0-5$) clusters have previously been the subject of the photoelectron experiments³ that allowed observation of the evolution of chemical bonding in sequential oxidation of Al_3O_y clusters starting from Al_3 . It was further argued that chemical bonding in anionic Al_3O_5 cluster is expected to be

similar to that in the bulk alumina. This is based on the assumption of the complete charge transfer of the Al valence electrons to oxygen atoms leading to Al^{3+} and O^{2-} ions in the cluster. One can therefore conclude that Al_3O_5^- emulates a complete oxide cluster.³ For the neutral Al_3O_5 cluster, the predicted ground state is a basket-like configuration in which 3-fold coordination of Al atoms is achieved by sharing of two oxygen atoms by two Al atoms. Starting from this configuration, one can then suggest the ground state of Al_3O_6 to be the configuration in which Al atoms are fully 3-fold coordinated without sharing O atoms. This is what has been predicted by DFT calculations for the ground state of neutral Al_3O_6 in the present study (Figure 2).

Once the total valency of the oxygen atoms exceeds that of the Al atoms, the cluster becomes electron deficient for the charge transfer to occur between Al and O atoms and shows preference for the formation of O–O bonds. In other words, an O_2 unit is expected to replace an oxygen atom in the oxygen-excess alumina clusters. In the present study, the predicted ground states for the neutral Al_3O_7 and Al_3O_8 consist of the

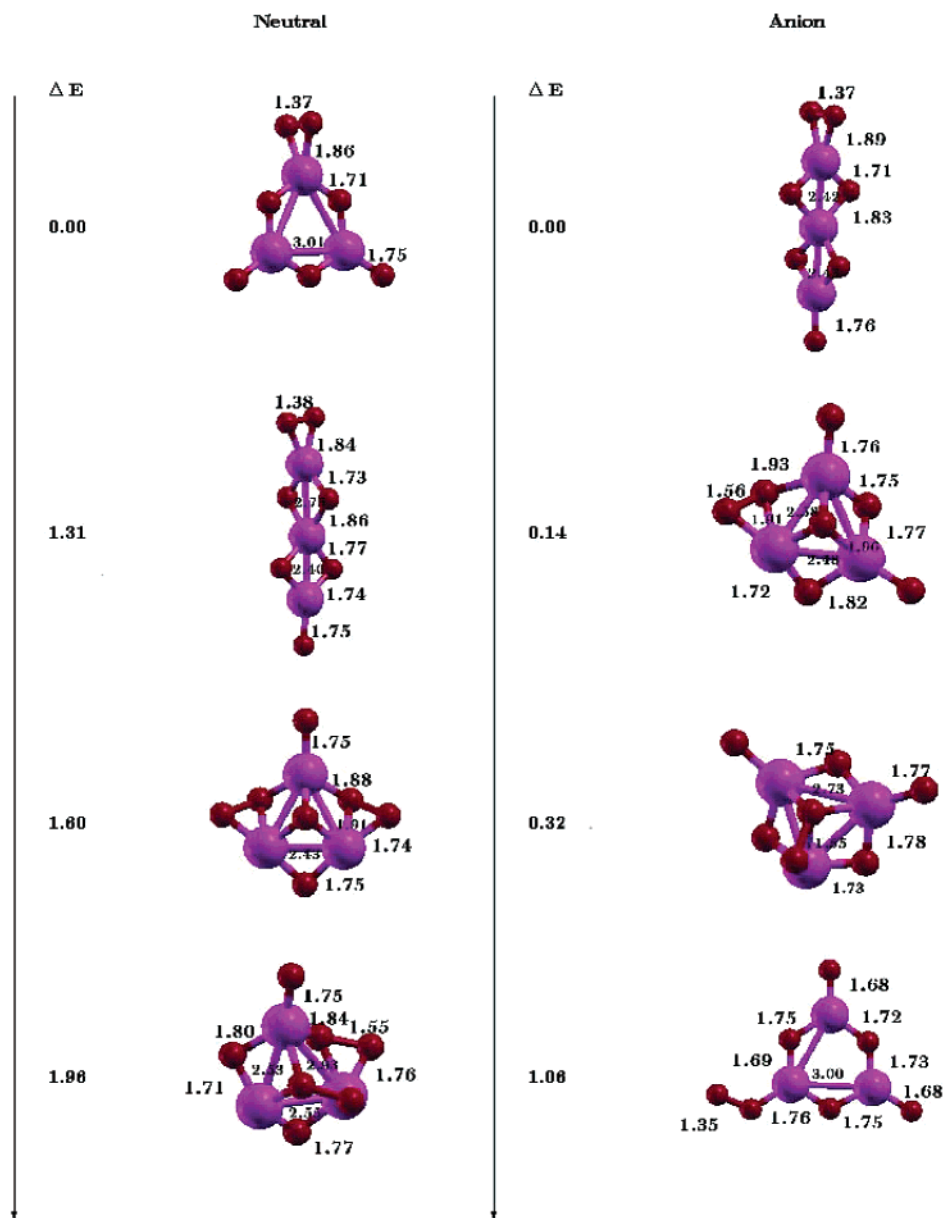


Figure 3. Some of the lowest energy configurations of neutral and anionic Al_3O_7 . Energy difference is in eV. Aluminum and oxygen atoms are represented by large and small filled circles, respectively.

structures with an O_2 unit, as shown in Figures 3 and 4. This is further reinforced by Mulliken population analysis of both neutral and anionic clusters, as discussed below.

B. Mulliken Population Analysis. Mulliken population analysis is commonly used to identify qualitative trends in the atomic charges and chemical bonding, though it does depend on the choice of basis sets used in electronic structure calculations. In neutral alumina clusters considered here, the charge associated with the Al atoms (q_{Al}) is about 1.04 e and remains the same for Al surrounded by either three O atoms (in Al_3O_6) or four O atoms (in Al_3O_8). On the other hand, the Mulliken charge for O (q_{O}) depends on its coordination in the cluster. The bridging O atom shared by two Al atoms has a charge of -0.70 e, while the terminating O atom has a charge of -0.34 e. When the terminating O atom is replaced by the O_2 molecule (e.g. Al_3O_8), the charge associated with each O atom in the molecule is -0.17 e, indicating an equal sharing of charge by two O atoms in the molecule. A similar trend in q_{Al} and q_{O} has been observed in the negatively charged Al_3O_7^- and Al_3O_8^- clusters.

In the bulk Al_2O_3 , q_{Al} and q_{O} are calculated to be $+1.13$ e and -0.75 e, respectively.³⁰ On the other hand, the DFT calculations find q_{Al} and q_{O} to be $+0.52$ e and -0.52 e (respectively) in the AlO molecule. It therefore appears that q_{Al} in neutral Al_3O_6 , Al_3O_7 , and Al_3O_8 clusters have reached the bulk limit of the Mulliken charge.

For anionic clusters, however, the predicted ground state neither shows a preference for the close-packed (basket-like) structures nor shows a preference for the closed-shell electronic configurations. The singlet–triplet splitting in the anionic clusters comes out to be about 1.6 eV, with the triplet being lower in energy. This is in contrast to the results for Al_3O_5^- , where the singlet spin state is preferred, though the ground-state configuration is different from that in the neutral state. Assuming that Al_3O_5^- is completely ionic, the available closed-shell orbitals are no longer enough to sustain the consumption of electrons of the additional O atom in Al_3O_6^- . Thus, higher spin multiplicity that forms an open-shell system is favored for higher oxygen content clusters. This is further reflected in the ground-state configuration, where Al atoms prefer a linear struc-

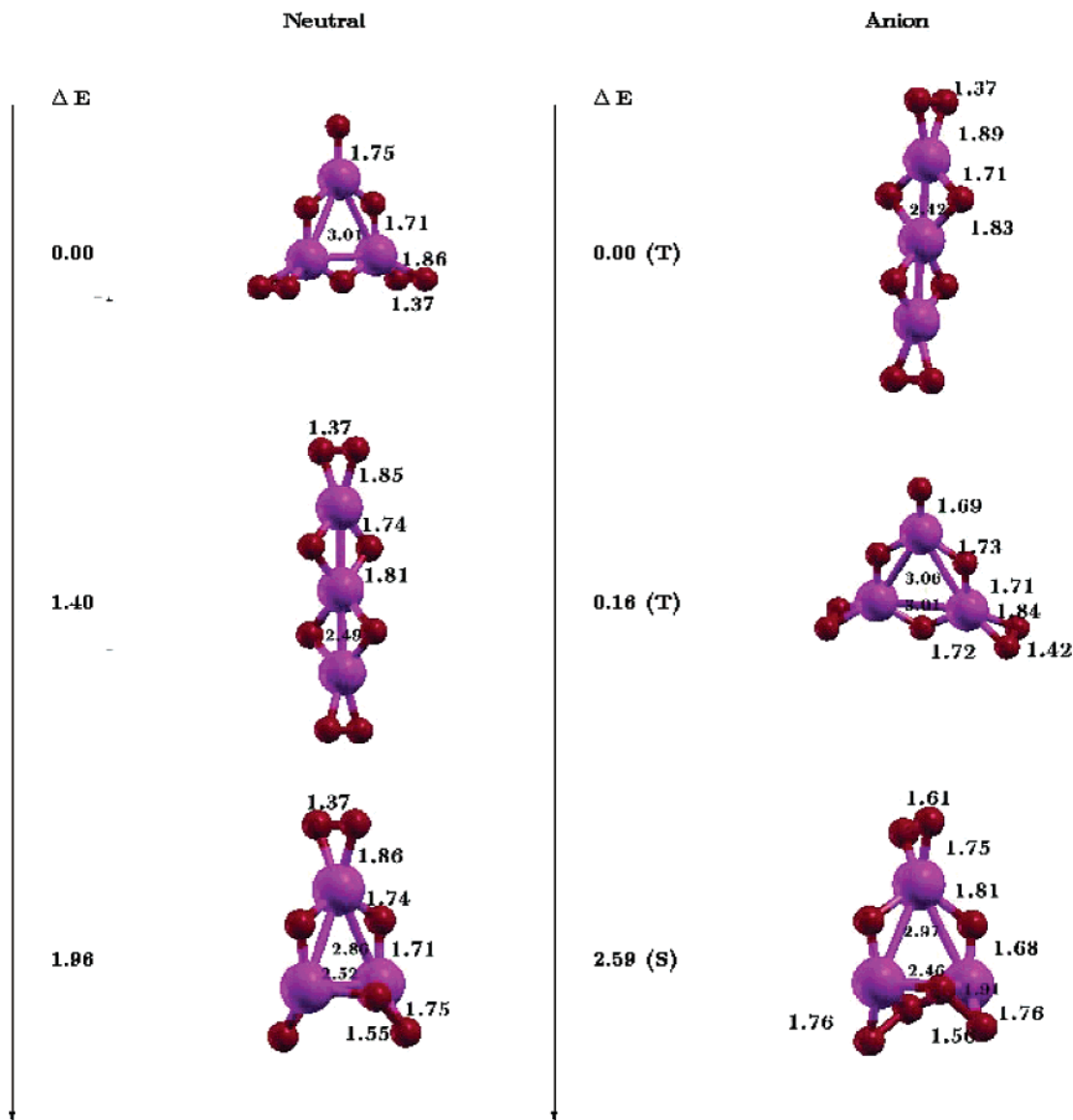


Figure 4. Some of the lowest energy configurations of neutral and anionic Al_3O_8 . Energy difference is in eV. Aluminum and oxygen atoms are represented by large and small filled circles, respectively.

ture instead of a trigonal planar geometry. This may facilitate the formation of additional chemical bonds and further orbital hybridization to form stable anionic cluster configurations.

The structural motif of the ground state of anionic clusters is predicted to be the twisted-pair rhombus, i.e., two Al_2O_2 units linked via a single Al atom, and the ground state changes from a planar to nonplanar configuration in going from Al_3O_6^- to Al_3O_8^- . However, we also note the presence of low-lying hexagonal isomers for both the Al_3O_6^- and Al_3O_8^- systems, each being only 0.16 eV above the ground-state structure (Figures 2 and 4). Curiously, the Al_3O_7^- anion, an analogous triplet structure of C_s symmetry, was 1.06 eV higher in energy. Instead, a highly condensed C_1 structure was calculated to be 0.14 eV above the ground state.

Mulliken charges of anionic clusters appear to provide a clue in explaining their preference for the twisted-pair rhombus structures over the basket (3D) structures. When we add an electron to neutral alumina clusters, the extra electron is expected to localize mainly on Al atoms, in accordance with chemical intuition. This is what we have found³⁰ for Al_3O_3^- , where the extra electron is mainly shared by Al atoms, changing q_{Al} from +0.74 e to +0.37 e upon addition of the electron. In the oxygenen-

excess alumina clusters (e.g. Al_3O_6^-), however, the O atoms are expected to play a relatively larger role in sharing the extra electron. The degree of sharing of the added electron by O atoms would therefore be expected to influence in the determination of the ground state of anionic oxygen-rich alumina clusters. Figure 5 displays q_{Al} and q_{O} of two low-lying isomers of the neutral and anionic Al_3O_6 cluster. Accordingly, the added electron mainly resides on the terminal O atoms in the planar hexagonal C_{2v} configuration, while both Al and O atoms approximately equally share the added electron in the twisted-pair rhombus structure. This difference in the charge distribution is further confirmed by Mulliken population analysis of neutral and anionic Al_3O_7 and Al_3O_8 clusters (not shown).

C. Stability. The stability of neutral alumina clusters with respect to their fragmentation into atoms and molecules will be considered here. We will use the total energy of the most stable isomers of Al_3O_6 , Al_3O_7 , and Al_3O_8 to calculate the binding and fragmentation energies. The binding energy is defined as the energy required to dissociate the cluster into atoms. All clusters seem to be very stable from a binding energy consideration. The values for the binding energy/atom are 4.21, 4.16, and 4.11 eV for Al_3O_6 , Al_3O_7 , and Al_3O_8 , respectively. Since

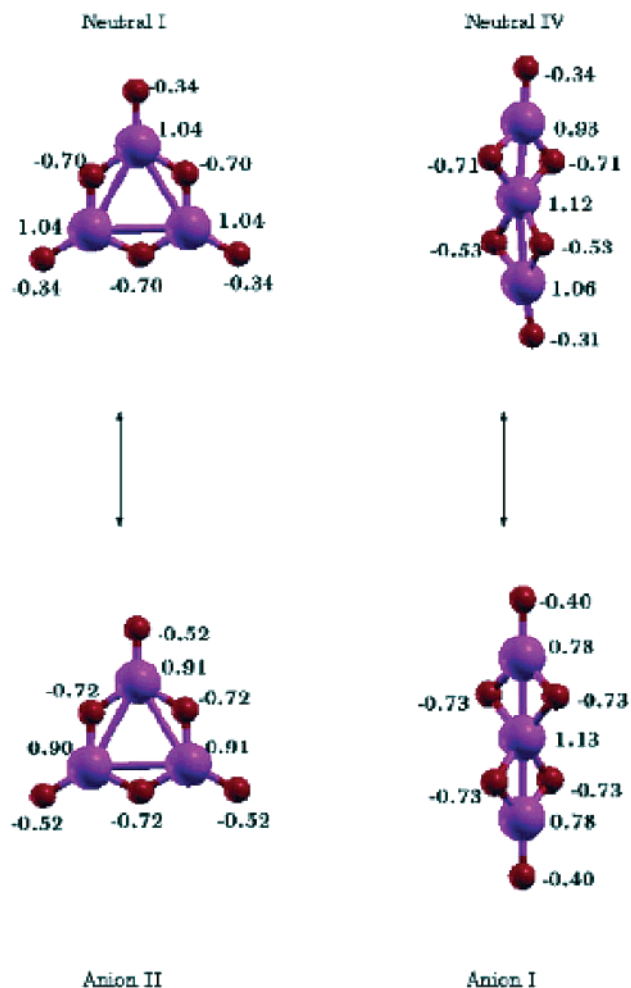


Figure 5. Schematic representation of Mulliken charges in neutral and anionic Al₃O₆.

TABLE 1: Fragmentation Energies (eV) for Al₃O_n ($n = 6-8$) Clusters^a

system	$n = 6$	$n = 7$	$n = 8$
Al ₃ O _n → 3Al + nO	37.9	41.6	45.21
Al ₃ O _n → Al ₃ O _{n-1} + O	6.53	4.76	6.42
Al ₃ O _n → Al ₃ O _{n-2} + O ₂		1.95	2.13
Al ₃ O _n ⁻ → Al ₃ O _{n-1} ⁻ + O	3.83	3.51	3.51
Al ₃ O _n ⁻ → Al ₃ O _{n-2} ⁻ + O ₂	3.62	1.94	1.61

^a The first fragmentation reaction corresponds to the binding energy.

the binding energy/atom for Al₃O₅ is calculated to be 4.28 eV, sequential oxidation of alumina clusters appears to decrease their stability slightly. The fragmentation channels considered here involve either an O atom or an O₂ molecule (Table 1). Although both neutral and anionic clusters show preference for the fragmentation via an O₂ molecule, they appear to be stable against fragmentation.

D. Vibrational Frequencies. To assess the stability of the ground state of neutral and anionic clusters, the vibrational frequencies were calculated and analyzed. Figure 6 shows the frequency spectrum of neutral and anionic Al₃O_n ($n = 6-8$) clusters in which the frequencies ranging from 52 to 1000 cm⁻¹ correspond to the movements of Al–O bonds. The frequencies of these clusters are expected to be similar to each other, because of their structural similarity. For Al₃O₇ and Al₃O₈, however, two distinct frequencies appear at about 420 and 1146 cm⁻¹, corresponding to movements of the O–O bond in the O₂ molecule. That the O–O frequency signature is not present in

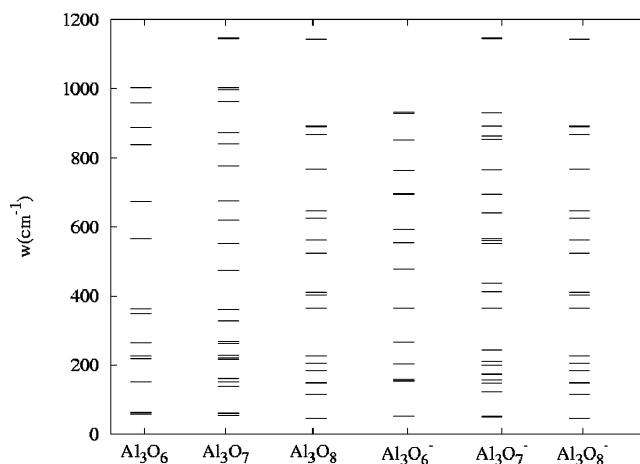


Figure 6. Vibrational frequency spectra of neutral and anionic Al₃O_n ($n = 6-8$).

TABLE 2: Vertical and Adiabatic Electron Affinity (eV) for Al₃O_n ($n = 6-8$) Clusters

system	electron affinity	
	vertical	adiabatic
Al ₃ O ₆ ⁻	5.04	3.56
Al ₃ O ₇ ⁻	4.96	3.44
Al ₃ O ₈ ⁻	4.88	3.32

Al₃O₆ further provides a proof that an O₂ molecule has replaced an O atom in Al₃O₇ and Al₃O₈. The vibrational frequencies of anionic clusters also show features similar to those found in the neutral clusters.

E. Electronic Properties. For the lowest energy isomers of Al₃O₆, Al₃O₇, and Al₃O₈, the HOMO–LUMO gap values are 3.65, 3.67, and 3.72 eV, respectively. For a series of Al₃O_n, one expects the electronic structure of the Al₃O_n clusters to become increasingly simple, because the valence electrons of Al are sequentially transferred to the O atoms. This is what we have observed in the calculated values of the HOMO–LUMO gap of the clusters considered here. The values are large and are representative of the insulating character of the bulk alumina. It is to be noted here that the experimental band gap of the bulk alumina is 8.7 eV.

In the photoelectron spectroscopy experiments on anions, the electron affinity of the corresponding neutral cluster is estimated by photodetachment of the electron from the ground-state geometry of the anion. So, to have a realistic comparison between our calculated values and experimental data, we define the vertical electron affinity (EA) of these clusters as the energy difference between the anionic and neutral clusters, both at the optimized geometry of the anionic cluster (i.e. EA = $E(q=0) - E(q=-1)$, where E is the total energy of the cluster and q is the charge of the cluster). Following this definition, the calculated electron affinity can also be termed as the *vertical electron detachment energy*. On the other hand, adiabatic EA values reflect the relaxation effects on the configuration after the removal of an electron. The vertical and adiabatic electron affinities (EA) for the alumina clusters are computed and given in Table 2.

Both vertical and adiabatic values of the EA show a small variation with the sequential oxidation of the alumina clusters considered here. These values are higher than the calculated value of 2.21 eV for the AlO molecule. The higher EA values for the oxygen-rich alumina clusters are expected and are a manifestation of the dominance of the oxygen orbitals in forming the HOMOs of neutral and anionic clusters. We are not aware

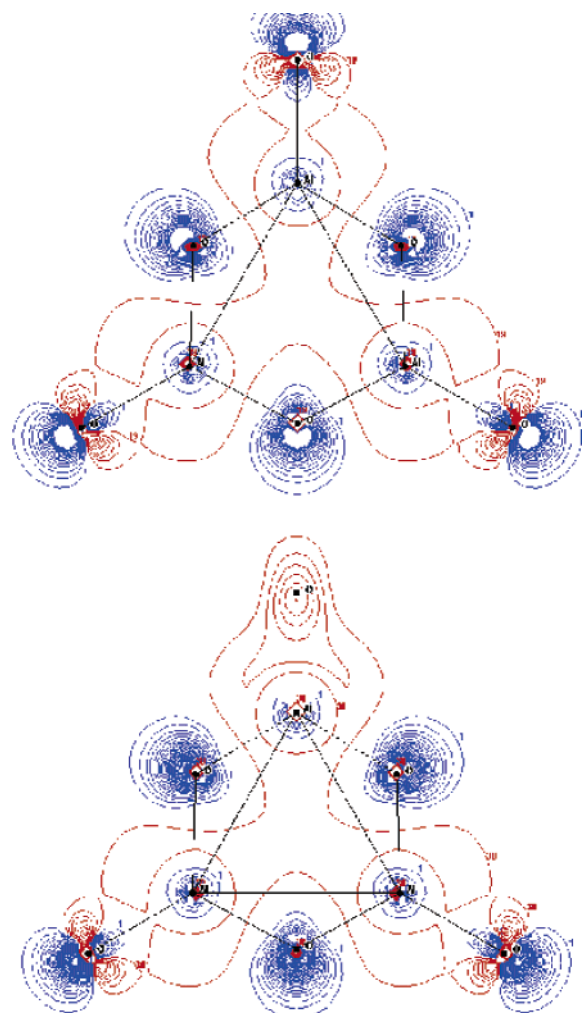


Figure 7. Difference charge-density, $\Delta\rho$, surfaces for the lowest energy structure of Al_3O_6 (upper) and Al_3O_7 (lower). The charge densities have been given for 0.01 electron/au respectively.

of any experimental or theoretical values of the electron affinity of Al_3O_6 , Al_3O_7 , and Al_3O_8 . We note here that the photoelectron experiments on Al_3O_5^- measured values of 5.21 and 4.92 eV for the vertical and adiabatic electron affinity, respectively. The calculated electron affinity increases from Al_3O_3 to Al_3O_6 , but after that it appears to slowly decrease.

It is convenient to investigate the bonding characteristic of a given cluster by examining the difference charge density represented by $\Delta\rho$, $\Delta\rho = \rho_{\text{scf}} - \rho_{\text{superimpose}}$, where, ρ_{scf} is the self-consistent density and $\rho_{\text{superimpose}}$ is the superimposed atomic charge density.

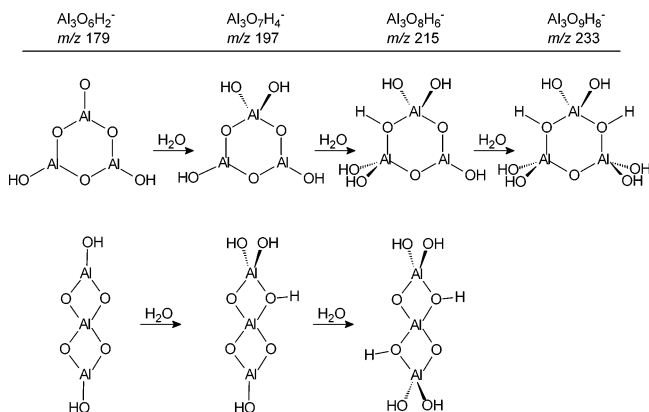
The isodensity surfaces for difference charge density of Al_3O_6 and Al_3O_7 are shown in Figure 7. The surfaces are plotted for the 2D Al_3O_3 hexagonal plane. The difference charge density plots clearly show the ionic character of the Al–O bond in these clusters. The bridging O atoms indicate the polarization of the electron density perpendicular to the Al–O bond, while the electron density of the terminal O atoms tend to polarize along the Al–O bond. A distinct feature in the isodensity surface of Al_3O_7 appears, showing the replacement of a terminal O atom by a terminal O_2 molecule; in this case, no electron density appears adjacent to the topmost Al atom, because the O atoms attached there are located above and below the hexagonal plane.

F. Experimental Results. Al_3O_n^- cluster anions could be formed in the gas phase by bombarding alumina surfaces using energetic (keV) ions as projectiles (i.e., secondary ion mass

spectrometry). In the SIMS spectrum of $\text{Al}(\text{OH})_3$ and other aluminum oxides, series of cluster ions are formed from bombardment of the surface. One of the more abundant series has the general formula $\text{Al}_n\text{O}_{2n}\text{H}_{n-1}^-$, and the three Al members have the formula $\text{Al}_3\text{O}_6\text{H}_2^-$ (m/z 179). The experimental SIMS employs a quadrupole ion trap mass spectrometer such that ion lifetimes are long enough to enable the reactivity of the molecules to be examined, particularly if reagent neutral molecules are added to the gas-phase atmosphere.

The formation of $\text{Al}_3\text{O}_6\text{H}_2^-$ afforded the opportunity to assess reactivity, which might allow correlation with Al_3O_6^- structures generated using DFT. Obviously, the presence of two H atoms in the experimental system could result in a perturbation of the relative energies calculated for Al_3O_6^- ; yet, if H atoms were merely used to satisfy the unoccupied valence of the pendant O atoms (Chart 1), then the twisted-pair rhombus and the planar hexagonal structures would still be expected to be energetically competitive. However, the reactivity of the two putative structures would be expected to be significantly different: The planar hexagonal isomer of $\text{Al}_3\text{O}_6\text{H}_2^-$ contains three under-coordinated Al atoms that would be expected to behave as Lewis acids, whereas the twisted-pair rhombus contains only two. Previous studies had shown that $\text{Al}_1\text{O}_n\text{H}_p^-$ and $\text{Al}_2\text{O}_n\text{H}_p^-$ could be examined via their reactivity with water.¹²

CHART 1



When $\text{Al}_3\text{O}_6\text{H}_2^-$ (m/z 179) was isolated in the IT-SIMS and then allowed to react with gaseous H_2O (Figure 8), three sequential hydration reactions were observed, forming $\text{Al}_3\text{O}_7\text{H}_4^-$ (m/z 197), $\text{Al}_3\text{O}_8\text{H}_6^-$ (m/z 215), and $\text{Al}_3\text{O}_9\text{H}_8^-$ (m/z 233). The reaction sequence proceeded to completion, forming m/z 233 only, but no evidence was observed for addition of a fourth H_2O molecule under our conditions. The result strongly supports the planar hexagonal structure: here, addition of H_2O is almost certainly dissociative, and thus, addition of each H_2O molecule would require the presence of an under-coordinated Al atom. Ab initio calculations by our group on $\text{Al}_2\text{O}_n\text{H}_p^-$ ¹² and by Wittbrodt on Al_4O_6 supported dissociative adsorption³¹ (although for the larger Al_8O_{12} cluster molecular adsorption was competitive³¹).

An alternative explanation might be that the twisted-pair rhombus undergoes ring opening upon H_2O addition, enabling a partially linear structure that would accommodate a third H_2O without necessitating a trigonal bipyramidal configuration for Al. In fact, we have recently observed slow addition of a third H_2O to rhombic $\text{Al}_2\text{O}_4\text{H}^-$, which would require just such a ring opening, and some ring opening is likely occurring in the hydration of Al_3O_5^- (see below). However, if this type of process were prevalent in the twisted-pair rhombic Al_3 system,

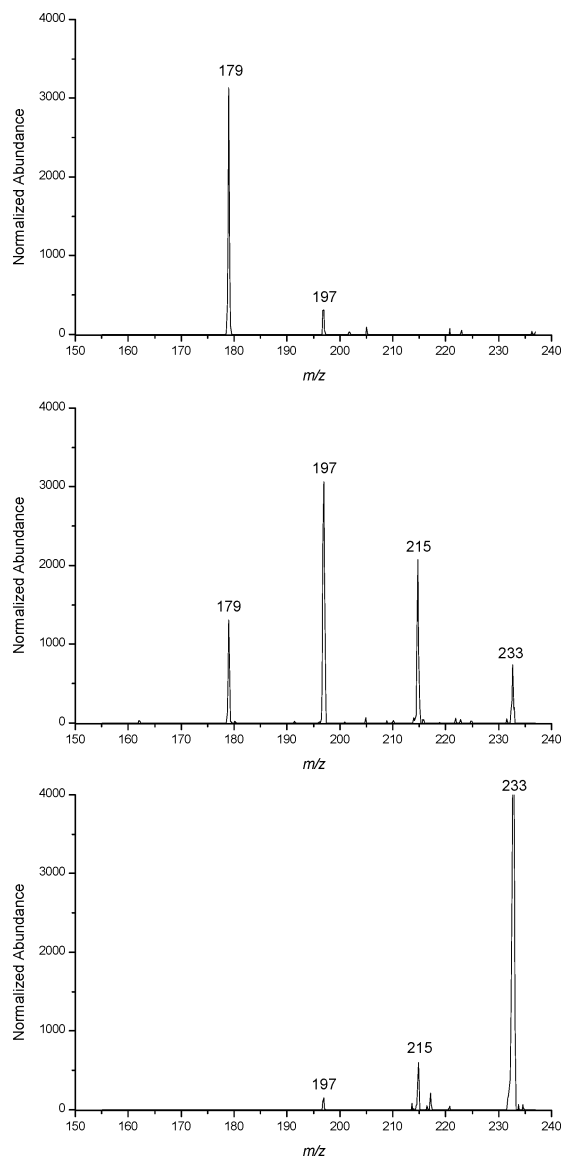


Figure 8. Anion IT-SIMS spectra for isolated ion m/z 179 hydration reaction of $\text{Al}_3\text{O}_6\text{H}_2^- + \text{H}_2\text{O}$ showing the addition of three H_2O molecules. Spectrum after 2 ms (top) reaction time; (center) after 32 ms; (bottom) after 302 ms. There was no evidence for addition of a fourth H_2O , even after the longest experimentally accessible reaction times (10 s).

then rupture of both rings might be expected, enabling formation of $\text{Al}_3\text{O}_{10}\text{H}_{10}^-$ at m/z 251, and this is not observed.

Hydration of Al_3O_5^- was also examined. This ion was formed via collision-induced dissociation (CID) of the $\text{Al}_3\text{O}_6\text{H}_2^-$ that was sputtered directly from the surface of the alumina. After formation, Al_3O_5^- was isolated and reacted with H_2O , whereupon it immediately converted to $\text{Al}_3\text{O}_6\text{H}_2^-$, which subsequently added three additional H_2O molecules. Hydration rate constants were comparable for $\text{Al}_3\text{O}_7\text{H}_4^-$ formed from $\text{Al}_3\text{O}_6\text{H}_2^- + \text{H}_2\text{O}$ and for $\text{Al}_3\text{O}_7\text{H}_4^-$ formed from $\text{Al}_3\text{O}_5^- + 2\text{H}_2\text{O}$,³² which suggests structural similarity, regardless of whether hydration starts from directly sputtered $\text{Al}_3\text{O}_6\text{H}_2^-$ or from Al_3O_5^- ; however, the observation does not provide further insight into structural possibilities for the Al_3O_6 system.

IV. Conclusions

A strong tendency to form the oxygen–oxygen bond is revealed in this study for neutral and anionic Al_3O_n ($n = 6–8$)

clusters. The calculated results show that 3D geometries are preferred over planar ones for neutral clusters. For anionic clusters, twisted-pair rhombus geometries are favored over the closed-packed ones, possibly due to delocalized distribution of the extra electron with a triplet spin state. The higher EA values for these oxygen-rich alumina clusters are the manifestation of the dominance of the oxygen orbitals in forming the HOMOs of anionic clusters. Both neutral and anionic clusters are stable against fragmentation via O atom or O_2 molecule.

The existence of two competitive Al_3O_6^- structures provides guidance for interpreting hydration behavior of $\text{Al}_3\text{O}_6\text{H}_2^-$ generated experimentally in an ion trap-secondary ion mass spectrometer. $\text{Al}_3\text{O}_6\text{H}_2^-$ undergoes three sequential hydration reactions, which supports a structure containing three under-coordinated Lewis acid sites, consistent with the triplet planar hexagonal structure calculated for Al_3O_6^- , which was only 0.16 eV above the lowest energy structure (the twisted-pair rhombus).

Acknowledgment. The authors would like to thank CSERI, MTU for providing computational resources for the study. S.G. acknowledges the support of the Dow Corning Foundation. A.K.G. and G.S.G. acknowledge support by the United States Department of Energy Environmental Systems Research Program under contract DE-AC-07-99 I.D.13727 BBWI.

References and Notes

- (1) Henrich, V. E.; Cox, P. A. *The Surface Science of Metal Oxides*; Cambridge University Press: New York, 1994.
- (2) Desai, S. R.; Wu, H.; Rohlffing, C. M.; Wang, L. S. *J. Chem. Phys.* **1997**, *106*, 1309.
- (3) Hongbin, W. F.; Li, X.; Wang, X. B.; Ding, C. F.; Wang, L. S. *J. Chem. Phys.* **1998**, *109*, 449.
- (4) Boldyrev, A. I.; Schleyer, P. v. R. *J. Am. Chem. Soc.* **1991**, *113*, 9045.
- (5) Zakrzewski, V. G.; Niessen, W. V.; Boldyrev, A. I.; Schleyer, P. V. R. *Chem. Phys. Lett.* **1993**, *174*, 167.
- (6) Martínez, A.; Tenorio, F. J.; Ortiz, J. V. *J. Phys. Chem., A* **2001**, *105*, 8787.
- (7) Martínez, A.; Tenorio, F. J.; Ortiz, J. V. *J. Phys. Chem., A* **2001**, *105*, 11291.
- (8) Martínez, A.; Sansores, L. E.; Salcedo, R.; Tenorio, F. J.; Ortiz, J. V. *J. Phys. Chem., A* **2002**, *106*, 10630.
- (9) Martínez, A.; Tenorio, F. J.; Ortiz, J. V. *J. Phys. Chem., A* **2003**, *107*, 2589.
- (10) Ghanty, T. K.; Davidson, E. R. *J. Phys. Chem., A* **1999**, *103*, 2867.
- (11) Ghanty, T. K.; Davidson, R. R. *J. Phys. Chem., A* **1999**, *103*, 8985.
- (12) Scott, J. R.; Groenewold, G. S.; Gianotto, A. K.; Benson, M. T.; Wright, J. B. *J. Phys. Chem., A* **2000**, *104*, 7079.
- (13) Groenewold, G. S.; Hodges, B. D. M.; Scott, J. R.; Gianotto, A. K.; Appelhans, A. D.; Kessinger, G. F.; Wright, J. B. *J. Phys. Chem., A* **2001**, *105*, 4059.
- (14) Frisch, M. J.; Trucks, G. W.; Schlegel, H. B.; Scuseria, G. E.; Robb, M. A.; Cheeseman, J. R.; Zakrzewski, V. G.; Montgomery, J. A., Jr.; Stratmann, R. E.; Burant, J. C.; Dapprich, S.; Millam, J. M.; Daniels, A. D.; Kudin, K. N.; Strain, M. C.; Farkas, O.; Tomasi, J.; Barone, V.; Cossi, M.; Cammi, R.; Mennucci, B.; Pomelli, C.; Adamo, C.; Clifford, S.; Ochterski, J.; Petersson, G. A.; Ayala, P. Y.; Cui, Q.; Morokuma, K.; Malick, D. K.; Rabuck, A. D.; Raghavachari, K.; Foresman, J. B.; Cioslowski, J.; Ortiz, J. V.; Stefanov, B. B.; Liu, G.; Liashenko, A.; Piskorz, P.; Komaromi, I.; Gomperts, R.; Martin, R. L.; Fox, D. J.; Keith, T.; Al-Laham, M. A.; Peng, C. Y.; Nanayakkara, A.; Gonzalez, C.; Challacombe, M.; Gill, P. M. W.; Johnson, B. G.; Chen, W.; Wong, M. W.; Andres, J. L.; Head-Gordon, M.; Replogle, E. S.; Pople, J. A. *Gaussian 98*, revision A.4; Gaussian, Inc.: Pittsburgh, PA, 1998.
- (15) Groenewold, G. S.; Scott, J. R.; Gianotto, A. K.; Hodges, B. D. M.; Kessinger, G. F.; Benson, M. T.; Wright, J. B. *J. Phys. Chem., A* **2001**, *105*, 9681.
- (16) Gianotto, A. K.; Hodges, B. D. M.; Benson, M. T.; Harrington, P. d. B.; Appelhans, A. D.; Olson, J. E.; Groenewold, G. S. *J. Phys. Chem., A* **2003**, *107*, 5948.
- (17) Gianotto, A. K.; Hodges, B. D. M.; Harrington, P. d. B.; Appelhans, A. D.; Olson, J. E.; Groenewold, G. S. *J. Am. Soc. Mass Spectrom.* **2003**, in press.

- (18) Gresham, G. L.; Gianotto, A. K.; Harrington, P. d. B.; Scott, J. R.; Olson, J. E.; Appelhans, A. D.; Groenewold, G. S. *J. Phys. Chem. A* **2003**, in press.
- (19) Gresham, G. L.; Groenewold, G. S.; Olson, J. E. *J. Mass Spectrom.* **2000**, *35*, 1460.
- (20) Groenewold, G. S.; Appelhans, A. D.; Ingram, J. C.; Gresham, G. L.; Gianotto, A. K. *Talanta* **1998**, *47*, 981.
- (21) Ingram, J. C.; Appelhans, A. D.; Groenewold, G. S. *Int. J. Mass Spectrom. Ion Processes* **1998**, *175*, 253.
- (22) Appelhans, A. D.; Delmore, J. E. *Anal. Chem.* **1989**, *61*, 1087.
- (23) Van Stipdonk, M. J.; Justes, D. R.; Santiago, V.; Schweikert, E. A. *Rapid Commun. Mass Spectrom.* **1998**, *12*, 1639.
- (24) Harris, R. D.; Van Stipdonk, M. J.; Schweikert, E. A. *Int. J. Mass Spectrom.* **1998**, *174*, 167.
- (25) Groenewold, G. S.; Delmore, J. E.; Olson, J. E.; Appelhans, A. D.; Ingram, J. C.; Dahl, D. A. *Int. J. Mass Spectrom. Ion Processes* **1997**, *163*, 185.
- (26) Dahl, D. A.; Appelhans, A. D. *Int. J. Mass Spectrom.* **1998**, *178*, 187.
- (27) *Practical Aspects of Ion Trap Mass Spectrometry*; Todd, J. F. J., Ed.; CRC Press: New York, 1995; Vol. 1, p 4.
- (28) Wang, L.; Nicholas, J. B.; Dupuis, M.; Hongbin, W.; Closson, S. D. *Phys. Rev. Lett.* **1997**, *78*, 4450.
- (29) Lengsfeld, B. H., III; Liu, B. J. *J. Chem. Phys.* **1982**, *77*, 6083.
- (30) Lau K C.; Gowtham, S.; Pandey, R. Unpublished results. (Bulk values for the Mulliken charges were obtained in the corundum phase using the Crystal98 program suite and DFT Hamiltonian (B3LYP) with the 6-31G* basis set. It was a typical periodic crystalline calculation in which long-range Coulombic interactions were included.)
- (31) Wittbrodt, J. M.; Hase, W. L.; Schlegel, H. B. *J. Phys. Chem., B* **1998**, *102*, 6539.
- (32) Gianotto, A. K.; Rawlinson, J. W.; Cossel, K. C.; Olson, J. E.; Appelhans, A. D.; Groenewold, G. S. *J. Am. Chem. Soc.*, in press.